Chemistry & Biology
Article

Rapidly Reversible Hydrophobization: An Approach to High First-Pass Drug Extraction

Sean D. Monahan,[1,*] Vladimir M. Subbotin,[1,*] Vladimir G. Budker,[2] Paul M. Slattum,[1] Zane C. Neal,[1] Hans Herweijer,[1] and Jon A. Wolff[2]
[1]Mirus Bio Corporation, 505 South Rosa Road, Madison, WI 53719, USA
[2]Departments of Pediatrics and Medical Genetics, Waisman Center, Medical School, University of Wisconsin-Madison, Madison, WI 53705, USA
*Correspondence: sean.monahan@mirusbio.com (S.D.M.), vladimir.subbotin@mirusbio.com (V.M.S.)
DOI 10.1016/j.chembiol.2007.08.011

SUMMARY

We have investigated a rapidly reversible hydrophobization of therapeutic agents for improving first-pass uptake in locoregional drug therapy. This approach involves the attachment of a hydrophobic moiety to the drug by highly labile chemical linkages that rapidly hydrolyze upon injection. Hydrophobization drastically enhances cell-membrane association of the prodrug and, consequently, drug uptake, while the rapid lability protects nontargeted tissues from exposure to the highly active agent. Using the membrane-impermeable DNA intercalator propidium iodide, and melphalan, we report results from in vitro cellular internalization and toxicity studies. Additionally, we report in vivo results after a single liver arterial bolus injection, demonstrating both tumor targeting and increased survival in a mouse tumor model.

INTRODUCTION

Attempts to improve the therapeutic index of drugs for tumor treatment have led to advancements in both prodrug design and drug-delivery systems [1–3]. Targeted delivery systems comprising liposomal, polymeric conjugate, micelle, polymeric micelle, and nanoparticles that employ active (receptor and antibody mediated) and passive (enhanced permeability and retention) tumor targeting have been described [4–13]. A particularly valuable component for the design of these advanced systems involves the use of hydrolytically or enzymatically labile chemical linkages, most notably *cis*-aconityl and hydrazones, in order to release the drug from the delivery system [7, 8, 14, 15].

Despite the advances in drug delivery, the treatment of liver tumors has remained problematic. The liver is the site of both primary tumors, such as hepatocellular carcinoma (HCC) and cholangiocarcinoma, and a variety of secondary metastatic malignancies [16, 17]. Traditional systemic chemotherapy has demonstrated poor antitumor benefit and only marginal increases in survival. As a result, resection and transplantation remain the only curative options, but a variety of factors often eliminate these possibilities [18–20]. These limitations have fostered the development of locoregional drug treatment strategies, such as direct hepatic artery infusion (HAI) and transcatheter hepatic artery chemotherapy (TAC) [21–26]. These approaches exploit the difference in the vascular supply of tumor and normal parenchyma; hepatic tumors are fed by a neovascularized hepatic arterial route, while the normal liver parenchyma is supplied mainly from the portal vein [27, 28]. Based on the idea of high first-pass drug extraction, drug delivery to the hepatic artery would result in the delivery of higher doses of drugs to the liver tumors, while decreasing normal hepatic tissue exposure, therefore minimizing drug-related toxicities [29, 30]. Unfortunately, despite the initial intrigue and several trials, the results to date have not been encouraging, even when combined with embolization in order to prolong drug contact with the tissue [31]. The limited benefit observed suggests that poor first-pass drug extraction by the tumor tissue remains a serious issue.

This report details the development of prodrugs with enhanced first-pass extraction, due to transient hydrophobic modification. Drug hydrophobization utilizing relatively stabile modifications such as esters and amides was shown to increase drug interactions with cellular membranes and has correlated with improved cellular uptake and lowered IC_{50} values [32–35]. However, concerns remain involving both compound aggregation and embolization, as well as the sequestering of the drug in the cell membrane [36]. In order to address these issues, we have developed a new approach, to our knowledge, to hydrophobization in which the drug is linked to a hydrophobic moiety by highly labile chemical linkages. Our results show that this approach, termed RRH for rapidly reversible hydrophobization, has great promise for selective first-pass extraction. Because the attachment linkages for the hydrophobic moieties are rapidly hydrolyzed, prodrug that is not extracted during a first-pass exposure rapidly reverts to the less membrane-permeable parent drug, enabling selective targeting of organs and tumors. The conceptual basis of this approach is presented in Figure 1.

We have investigated the modification and delivery of propidium iodide (PI), a non-membrane-permeable DNA

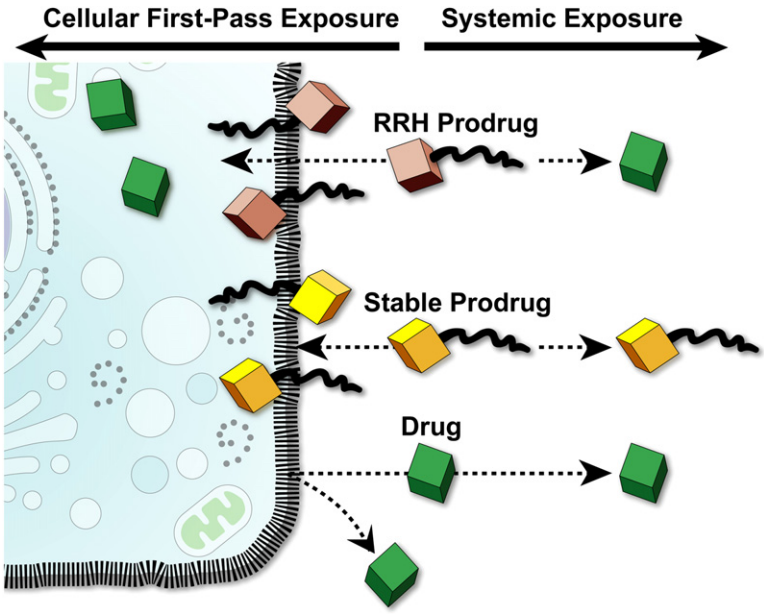

Figure 1. A Conceptual Schematic of the Cellular Delivery of a RRH Prodrug, a Stable Prodrug, and a Standard Drug
In the context of first-pass extraction, the RRH prodrug provides high levels of membrane attachment and internalization, while the prodrug that was not extracted reverts to the less membrane-active drug form. The hydrophobically modified prodrug with a stable linkage provides high levels of membrane attachment, followed by internalization by endocytosis. However, prodrug not extracted in a first-pass setting is still membrane active to other cells and tissues not being targeted. The drug itself has little cellular uptake and is available to other cells and tissues systemically.

intercalator, as a fluorescent reporter drug, and the antitumor agent melphalan. Hydrophobization of PI with very labile hydrophobic moieties substantially increased its entry into cells both in vitro and in vivo. Increased cellular uptake led to dramatically lower IC_{50} values in vitro. Hydrophobization of melphalan lowered IC_{50} values in vitro. We further report that a single liver arterial bolus injection of a RRH-PI prodrug significantly increased survival in a mouse MC38 liver tumor model.

RESULTS

The goal of RRH prodrugs is to increase the therapeutic index of drugs for first-pass extraction by creating a membrane-permeable compound for a very limited time. We reasoned that hydrophobization could be utilized to increase the drug's affinity for membranes and thereby increase drug-uptake levels. In essence, hydrophobicity is utilized as a means of cell targeting. By incorporating rapid lability into the hydrophobic system, we hoped to both reduce the possibility of embolization after delivery and exclude targeting of remote tissues, thereby limiting systemic exposure. Conceptually, the prodrug should only survive long enough to reach and treat the tissue of interest and should revert to the parent drug prior to encountering other remote tissues. In order to further limit drug uptake in these nontargeted cells, an ideal drug candidate would exhibit good cellular uptake as the hydrophobic prodrug and relatively little cellular uptake in its native form.

In order to test this idea of RRH modification on a membrane-impermeable compound, we chose to conduct our initial investigation on the DNA intercalator propidium iodide (PI). PI does not traverse uncompromised cell membranes, a property that is the basis of its widespread application as an indicator of cell viability. Additionally, PI exhibits a 20- to 30-fold enhanced fluorescence upon intercalation into DNA, facilitating detection of PI-positive cells. As a DNA intercalator, PI could also induce cytotoxicity by interfering with DNA replication and transcription [37, 38]. Chemically, PI possesses two amino groups at the three and eight positions of the phenanthridinium ring system that are available for modification (Figure 2).

Chemical Synthesis and Lability of RRH Prodrugs

Studies involving the basicity and modification of the 3,8-amino groups of ethidium (a closely related phenanthridinium) have demonstrated that the exocyclic amines are poor nucleophiles and weak bases (pKa = 0.8 and 2), necessitating the use of highly reactive electrophiles [39]. In the case of PI, we expected similar reactivity, and we therefore investigated two different approaches for labile hydrophobization. In the first approach, attachment of two octadecyl chains to PI was accomplished by the reaction of PI and chloro(dimethyl)octadecyl-silane (DMODSiCl) under basic conditions in either DMSO or DMF, affording the bis-silazane **II** in essentially quantitative yield after precipitation with diethyl ether (Figure 2). Although silazanes are well known, this modification has found only limited utility, in part due to rapid hydrolysis [40]. We believed, however, that this hydrolytic instability could be taken advantage of in our approach, if the prodrug could survive long enough to reach tissues of interest. Two additional compounds, a trisilylated PI and the anilinium salt of **II**, were identified as minor components in some of the reaction mixtures by ^{1}H-NMR (<10%). These compounds would be expected to show similar hydrolysis properties as **II**, and they were therefore not thought to be significant contaminants. Mass analysis of **II** indicated the mass for PI (and fragmentation products), presumably due to the hydrolysis during analysis.

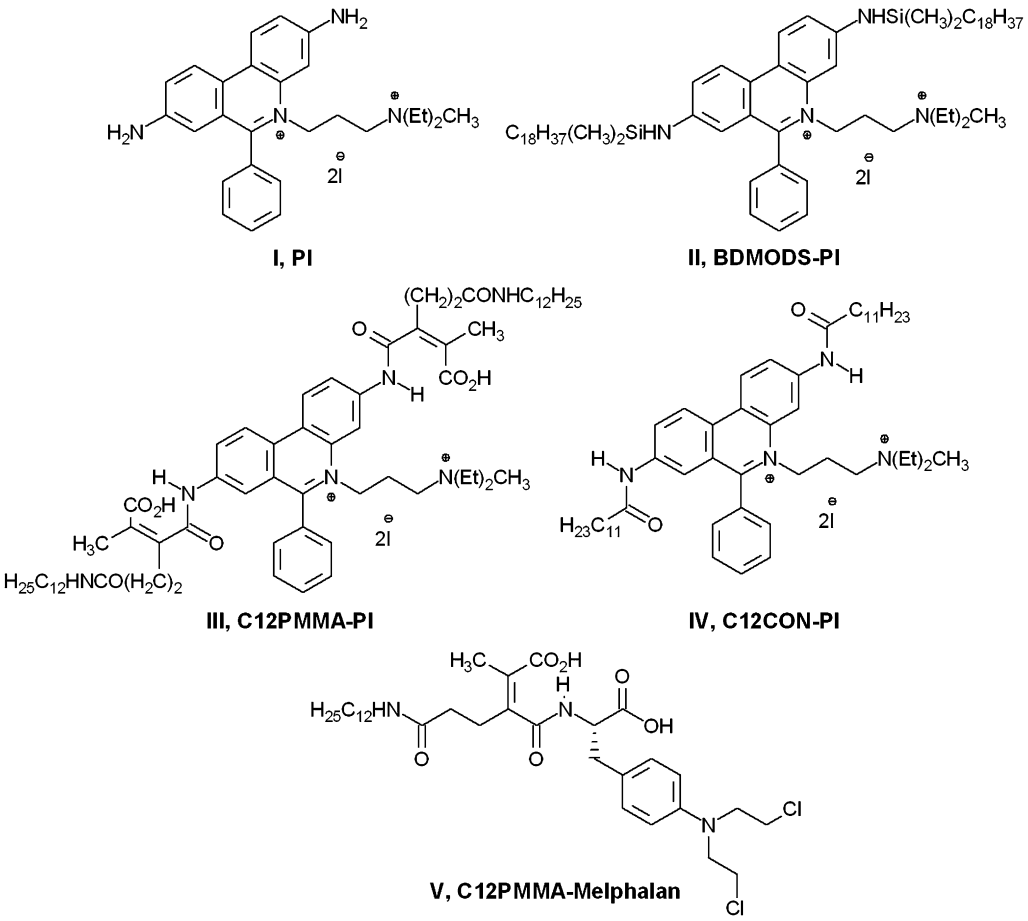

Figure 2. Structures for PI, PI Derivatives, and Melphalan Derivatives

A second modification approach utilized an amidation reaction between PI and the disubstituted maleic anhydride derivative N-dodecyl-3-(4-methyl-2,5-dioxo-2,5-dihydro-furan-3-yl)-propionamide (C12PMMA), to form the bis-maleamic acid **III** (Figure 2) as a mixture of isomers (arising from the amidation and ring-opening reaction occurring on either of the carbonyl groups of the cyclic anhydride). Maleamic acids are known to be labile under acidic pH, reverting to the amine and the cyclic anhydride; the derivatives of disubstituted maleic anhydride shows the most rapid rate of hydrolysis ($t_{1/2}$ = ~5 min at pH 5) [41]. Recent publications have detailed the use of hydrophobic maleic anhydride derivatives similar to C12PMMA for the reversible aqueous lipidation (REAL) of peptides, resulting in improved oral bioavailability [42, 43]. Although unstable at acidic pH, it was suggested that the REAL peptide survived the acidity encountered in the stomach due to precipitation of the derivative at acidic pH. In our system, however, we believed that the decreased nucleophilicity of the PI exocyclic nitrogens relative to aliphatic amines would result in a greatly enhanced rate of hydrolysis for **III** relative to the previously studied derivatives.

In order to test the effect of the rapid lability in our system, we also constructed a stable hydrophobic derivative of PI. Amidation of PI with lauroyl chloride was conducted, affording **IV** in 96% yield (Figure 2). The use of **IV** as a control compound in our uptake studies was facilitated by its fluorescent detection in the fluorescein channel. In order to test the effect of reversible hydrophobization with a known chemotherapeutic in a first-pass setting, we also modified melphalan with C12PMMA to afford maleamic acid, **V** (Figure 2). Based on amine pKa (melphalan pKas = 9.13 and 1.83; [44]), we expected that **V** would hydrolyze slower than the corresponding PI derivative, **III**.

The prodrugs were tested for their rate of hydrolysis at pH 6.0, 7.2, and 8.5 by using fluorescent spectroscopy (Table 1). Hydrophobization of PI resulted in a shift in the excitation maximum and a decrease in the measured fluorescence of the RRH-PI. Upon the addition of aqueous buffer to **II** or **III**, there was a rapid increase in fluorescence, indicating the loss of the hydrophobic group and reversion of the RRH-PI to unmodified PI. The silazane **II** was hydrolytically unstable, with a calculated $t_{1/2}$ of 23 s at pH 8.5. As the pH of the buffer was decreased to pH 7.2, the rate of hydrolysis increased ($t_{1/2}$ = 11 s). A similar

Table 1. Half-Life Values for RRH-PI and Melphalan Prodrugs

	Half-Life (k)		
Compound	pH 8.5	pH 7.2	pH 6.0
II	23.1 s (1.80 min^{-1})	10.5 s (3.96 min^{-1})	
III	21.1 s (1.97 min^{-1})	8.24 s (5.05 min^{-1})	
IV	nonlabile	nonlabile	
V			25.7 s (1.62 min^{-1})

trend was observed for **III**, with $t_{1/2}$s of 21 s (pH 8.5) and 8 s (pH 7.2). Hydrolysis of **V** was monitored by the reaction of the liberated melphalan with fluorescamine, resulting in a $t_{1/2}$ of 26 s at pH 6.0.

In Vitro Cellular Uptake Studies

Due to the instability of the RRH-PI prodrugs in water, it was necessary to dissolve them in a small amount of organic solvent (OS) and mix them with an aqueous solution immediately prior to delivery. There is precedence (for example, Onyx Liquid Embolic System) for the use of an OS in drug delivery. Rapid and efficient mixing was critical in order to avoid cellular damage or toxicity from the OS. Damaged cells would indicate successful PI uptake, interfering with the analysis of drug hydrophobization. We therefore constructed a small passive mixing chamber with colliding flows that utilized two syringe pumps for solution delivery (Figure 3A) [45, 46]. Testing with this mixing chamber (PI in DMF and isotonic glucose) resulted in very little PI uptake in cells, and results were comparable to those from control experiments in which an aqueous solution of PI (no OS) was added to the cell media. This indicated that the chamber was effective at mixing the solutions, resulting in no cellular PI uptake due to OS-mediated toxicity. This mixing chamber was utilized in all of the described experiments.

PI and the RRH-PI prodrugs were tested for cellular uptake on several cell lines, including B16 (murine melanoma), Hepa 1-6 (mouse hepatoma), SKOV-3 (human ovarian carcinoma), OVCAR-3 (human ovarian carcinoma), Jurkat (human T-lymphocyte), 293 (human embryonic kidney), and MC38 (mouse colon carcinoma) cells. Figures 3B and 3C show representative results after the application of PI and **II** to Hepa 1-6 cells. Unmodified PI stained very few cells (Figure 3B), while **II** yielded strong nuclear staining in all of the cells (Figure 3C). With longer camera exposure times, fluorescent signal could also be detected within the membrane and cytoplasm of the cells exposed to **II** (cytoplasmic PI is not as fluorescent as the nuclear, DNA-intercalated PI), but not in cells exposed to PI. Microscopic examination indicated that the cells that took up **II** appeared to be morphologically intact. Similar results were observed after the treatment of SKOV-3 cells (Figures 3D and 3E). **II** that was hydrolyzed by premixing with ITG (5 min) before application to the cells again resulted in very few PI-positive cells (identical to treatment with PI, data not shown), indicating that both prodrug hydrolysis and the liberated hydrophobic moiety did not contribute to PI uptake. The RRH prodrug **III** was similarly investigated for cellular uptake, and, in all cases, the results paralleled those obtained with **II** (data not shown). Additionally, results from the application of PI, **II**, and **III** on other cell lines (OVCAR-3, Jurkat, 293, and MC38) were similar to those detailed for the Hepa and SKOV-3 cell lines, indicating that internalization of the RRH-PI was not cell type specific.

Flow cytometry was used to quantitate prodrug delivery to Jurkat cells. Flow cytometry of cell suspensions that were treated with PI in aqueous solution (no OS, no mixing chamber) indicated very low PI uptake in most cells, with very few displaying a signal above 100 (0.3% ± 0.1%, control runs 1–4, Figure 3H). For cells that were suspended in ITG, and passed through the mixing chamber with unmodified PI (in DMSO), few PI-positive cells were observed (8.4% ± 0.6%, PI runs 1–4). However, when the same experiment was conducted with **II** in DMSO, flow cytometry indicated that nearly all cells were PI positive (99.5% ± 0.1%, **II** runs 1–4). These results were supportive of the large influence that hydrophobization had on PI internalization and correlated well with our observations by fluorescent microscopy.

The stable derivative **IV** was also tested for cellular uptake in SKOV-3 cells (Figures 3F and 3G). Immediately after application of **IV** to cells, a diffuse signal was observed along the cell membrane in the fluorescein channel (Figure 3F). No fluorescent signal was observed within the cytoplasm of the cell, even with longer camera exposure times. After a 1 hr incubation, a more defined punctate signal was observed (Figure 3G), likely due to endocytosis of the membrane-bound derivative. This indicated that hydrophobicity aided in membrane association, but that, in the absence of lability, the hydrophobic prodrug was sequestered and retained in the membrane.

In an attempt to clarify the cellular internalization of RRH-PI, several experiments were conducted. One possibility was that the prodrug induced membrane damage or acute toxicity, leading to drug internalization by diffusion, due to its amphipathicity. Hepa 1-6 cells were treated with **II** and then with Calcein AM (live cell marker). Approximately 86% of the cells were both PI and calcein positive, indicating viable cells (Figure 3I). Alternatively, Hepa 1-6 cells were treated with **II** and then with SYTOX Green (dead cell marker), resulting in less than 5% of cells being both PI and SYTOX Green positive (data not shown). When PI was added to SKOV-3 cells at the same time as **IV** or **V**, PI uptake by the cells was comparable to

controls (no **IV** or **V**). Lastly, a trypan blue assay for membrane disruption indicated that neither **V** nor methyl aniline silylated with chloro(dimethyl)octadecyl-silane caused generalized membrane disruption (data not shown). Based on these results, the hydrophobic agents do not appear to assist in the cellular entry of another molecule, suggesting that internalization is not due to generalized membrane damage.

Structurally, we thought that micelles could be generated upon mixing of the prodrug with the aqueous solution. Analysis of **IV** (after mixing with ITG) by dynamic light scattering indicated the formation of 36 nm particles (range = 28–42 nm, 18.3 Mcps). Similarly, dynamic light scattering analysis of **V** (after mixing with ITG) indicated the formation of 36 nm particles (range = 36–66 nm, 2.1 Mcps). Instability in aqueous solution and absorption of laser light (λ 533 nm) prevented direct measurement of RRH-PI prodrugs **II** and **III** by dynamic light scattering. Samples were therefore analyzed qualitatively for the presence of particles by measuring the 90° light scattering. Examination of **IV** (positive control) indicated a 15-fold increase in signal intensity relative to ITG or PI in ITG. However, the analysis of **II** and **III** by 90° light scattering indicated a maximum 2-fold increase in signal intensity relative to PI. Based on these results, we cannot definitively establish the presence of RRH-PI prodrug micelles. Given that the stable derivative **IV** and the melphalan derivative **V** did indicate the presence of micelles, it is probable that micelles, although transient in nature due to the rapid lability of the prodrug, do form for the RRH-PI prodrugs.

In Vitro Cytotoxicity

In order to investigate the effects of labile hydrophobization with C12PMMA on cytotoxicity, we tested melphalan and the prodrug **V** on Hepa 1-6, MC38, and SKOV-3 cells under conditions designed to mimic first-pass exposure. Cells were exposed to varying concentrations of **V** in DMSO for 4 min, and the cultures were assayed for viability (WST-1, Dojindo Molecular Technologies) after 48 hr. In Hepa 1-6 cells, the viability assay indicated an IC_{50} of 330 μM (±93 μM) (Table 2). Treatment with melphalan had a slight effect, with 81% (±2.3%) cell viability at the highest concentration tested (1458 μM). Previous studies have indicated that lower concentrations of melphalan caused higher cellular toxicity, but our experiments used shorter times for drug exposure (4 min versus 48 hr) in order to model first-pass exposure [47]. No toxicity was observed from the DMSO/ITG vehicle alone. **V** that was premixed with ITG containing 20 mM HEPES buffer (pH 6.5) (10 min) to hydrolyze the prodrug before application to the cells resulted in cell viability levels similar to those observed with melphalan. Similar toxicity profiles were observed in SKOV-3 and MC38 cells (Table 2).

Cell proliferation/toxicity studies were also conducted by using RRH-PI compounds (Table 2). In Hepa 1-6 cells, the viability assay at 24 hr posttreatment indicated an IC_{50} of 282 μM (±62 μM) for **II** (Table 2). PI had little effect, with 100% (±3.0%) cell viability at the highest concentration tested (1.25 mM). At 48 hr posttreatment, the viability assay indicated an IC_{50} of 334 μM (±72 μM) for **II**, while PI again had little effect at the highest concentration tested (93% ± 5.7% cell viability at 1.7 mM). **II** that was premixed with ITG (10 min) before application to cells resulted in levels of cell viability that were similar to those of the PI-treated cells (108% ± 1.3% at 833 μM). The stable PI derivative **IV** was also tested for toxicity in Hepa 1-6 cells at 24 and 48 hr posttreatment, resulting in IC_{50}s of 585 (±279 μM) and 429 μM (±37 μM), respectively. The toxicity resulting from **IV** may have been the result of endocytosis of the prodrug (hydrolysis of the amide would then yield PI), or its cationic amphipathic property. Similar results were obtained with SKOV-3 cells (Table 2).

In Vivo Delivery of RRH-PI Prodrugs

Encouraged by results from both the cellular uptake and cytotoxicity studies, a tumor model was established in mice with MC38 cells. Pathological evaluation was performed on select animals from each experimental group prior to testing to ensure arterialization of hepatic tumors and minimal signs of necrosis/apoptosis. After 2–3 weeks of tumor development, PI and RRH-PI were delivered via a liver arterial bolus injection (LABI). Due to the small diameter of the hepatic artery and its contraction after injection (leading to thrombosis), solutions were delivered to the right gastroduodenal artery for retrograde delivery to the hepatic artery. After 5 min, the livers were harvested, sectioned, and analyzed by fluorescent and confocal microscopy. Injection of **II** (0.150 μmol in 20 μl DMSO/200 μl ITG) resulted in strong PI-positive nuclear staining of MC38 liver metastases, but very little PI staining in normal liver parenchyma (Figures 4A and 4B). Hepatic arteries and some cells in the portal triads were also PI positive (Figure 4A, arrowhead), as were a few cells at the parenchyma-metastasis interface. No PI-positive cells were observed in any other organ examined (heart, lung, spleen, and kidneys) in any of the animals treated with **II**, indicating that **II** was hydrolyzed back to PI prior to encountering other tissues. LABI with **III** resulted in a similar cellular uptake pattern to that observed with **II** (data not shown). LABI with PI or **II** that was premixed with ITG (10 min) resulted in a relatively few PI-positive cells within the MC38 metastases, presumably necrotic or apoptotic cells (Figure 4C). Samples examined by confocal microscopy indicated a similar signal pattern (Figures 4G–4J).

Confocal imaging was also utilized to approximate the numbers of PI-positive cells after LABI in three different regions of the liver: Region 1, MC38 metastases; Region 2, portal triad areas; and Region 3, parenchyma representing zone 2 of the hepatic unit. LABI with **II** resulted in an average of 94% of the cells in Region 1 being PI positive. In Region 2, an average of 23% of the cells were PI positive. Positive cells in this region were comprised of arterial cells, some adjoining hepatocytes, and bile duct cells (all of which are exposed to **II** during the injection). In Region 3, an average of 1% of the cells were PI positive. These data were used to estimate the overall percentage of non-tumor cells in the liver that were PI positive. As Region 2

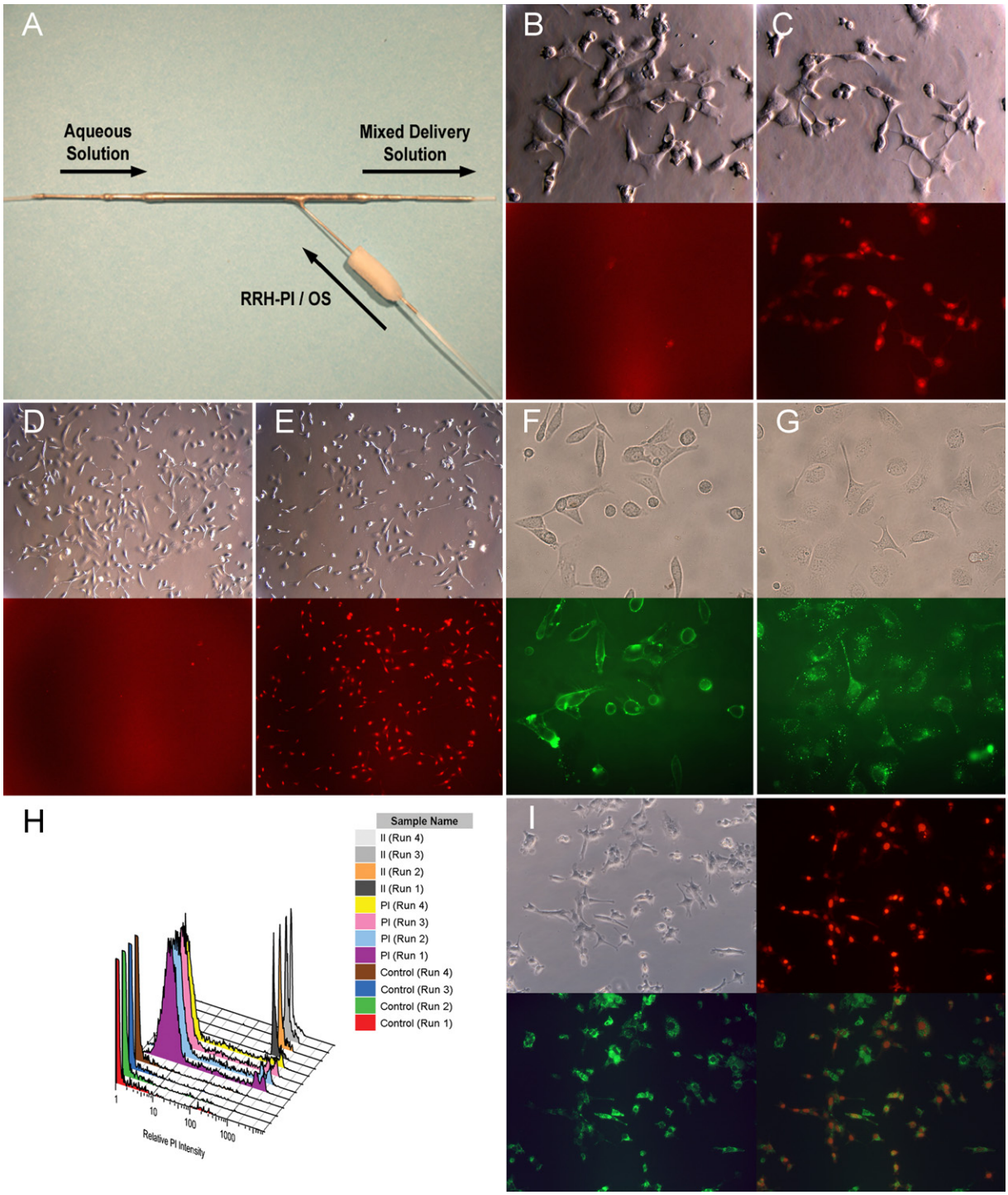

Figure 3. Delivery of PI, II, and IV to Various Cell Cultures

(A) The aqueous solution and the RRH prodrug in OS are delivered to the chamber by independent syringe pumps, with passive mixing from colliding flows.

(B–E) (B and D) PI or (C and E) **II**, 20 μl of 7.48 mM solution in DMSO, was mixed with ITG (200 μl) and added to the (B and C) Hepa 1-6 cells (magnification = 320×) or (D and E) SKOV-3 cells (magnification = 100×). After 30 s, the drug solution was removed, and 2 ml growth media was again added to the cells. The cells were immediately imaged with an Axiovert S100 fluorescent microscope (Zeiss), and the same fields were imaged with phase-contrast illumination and in the rhodamine fluorescence channel.

(F and G) SKOV-3 cells were treated with **IV** (20 μl 7.48 mM solution in DMSO) and (F) immediately imaged on an Axioplan-2 fluorescent microscope (Zeiss), or (G) incubated for 1 hr prior to imaging. The same fields were imaged with phase-contrast illumination and in the fluorescein fluorescence channels, magnification = 320×.

comprises less than 5%–7% of the liver (in humans, similar in rodent) [48], the total number of PI-positive nontumor cells in the liver can be estimated to be 2%–3%.

In order to evaluate tumor cell and hepatocyte uptake based on differences in vascular supply, RRH-PI prodrug was delivered into the portal vein of normal and tumor-bearing mice. No clamping of liver outflow was performed in order to avoid pressure-induced delivery [49]. Intraportal injection of **II** to tumor-bearing mice with preserved portal blood flow resulted in no signal within the metastases, and few hepatic and single nucleated blood cells being positive for PI (Figure 4D), likely due to RRH-PI being sequestered by blood constituents [50]. When intraportal delivery was performed with the portal vein and celiac artery transiently clamped to occlude blood flow, there was prominent labeling of portal structures and adjacent cells, including hepatocytes (Figure 4E), but not of the metastases. As with arterial injections, injection of unmodified PI into the portal vein (with occluded blood flow) resulted in a few labeled cells, either within the portal structure or hepatocytes (Figure 4F).

Analyses of cell suspensions prepared from normal liver samples after portal vein injections (occluded blood flow) of **II** resulted in ~70% of the hepatocytes being PI positive. Corresponding injections of PI resulted in ~1% of the cells being PI positive. Nucleic acid (DNA and RNA) isolated from the cell suspensions was analyzed by fluorescent spectroscopy, indicating that 1.2% of the injected PI was bound, as compared to 14% for **II**. This analysis accounts for PI that was bound to the nucleic acid in the hepatocytes, and not to PI that was still associated with the membrane or unbound within the cell, which would have been lost during nucleic acid isolation.

In addition to the MC38 model, we also performed preliminary testing of RRH-PI delivery in other relevant syngeneic murine liver metastases models, including Hepa 1-6 (hepatoma), B16 (melanoma), and NXS2 (neuroblastoma) utilizing LABI. Similar levels of PI-positive cells were observed; preferential staining of hepatic metastases and very minimal involvement of parenchymal cells was seen (data not shown). Additionally, in all cases, the results with **III** paralleled the results detailed with **II** (data not shown). Taken together, these results supported our idea that the RRH approach enabled selective and first-pass delivery of a drug to a tumor in vivo.

In Vivo Antiproliferative Effect

PI and **III** were intraportally injected (occluded blood flow) into normal mice immediately after a 70% hepatectomy in order to evaluate their effect on rapidly proliferating tissue. At 2 days after treatment with PI, an average of 7.0% (±2.2%) of the hepatocytes were in metaphase. In contrast, after treatment with **III**, an average of 2.3% (±2.9%) of the hepatocytes were in metaphase. Further studies were therefore conducted to determine whether **III** could have an antitumor effect on mice bearing MC38 liver metastases (Figure 5). In this study, hydrolyzed C12PMMA-PI (by premixing with ITG) was injected by LABI as a control. Animals that received **III** exhibited increased survival ($\rho = 0.02$), compared to the animals that received the hydrolyzed C12PMMA-PI (HyC12PMMA-PI, Figure 5), although survival was limited to a few days.

DISCUSSION

The conceptual basis of RRH prodrugs involves the use of labile hydrophobicity to aid in cell uptake in a first-pass delivery setting. While there are a variety of drugs with modifiable groups that could be delivered to cells in this fashion, antitumor compounds are one class of drugs that are suited to the RRH-based, first-pass approach. In particular, given the unique vascular architecture of the liver, with portal blood supplying most normal hepatic tissue and hepatic arterial blood supplying tumors within the liver, the locoregional delivery of RRH therapeutics is uniquely suited to the treatment of primary and metastatic liver neoplasms.

Using PI as a reporter molecule, RRH modification enabled PI's uptake into almost 100% of the cells in culture (Figure 3) and ~94% of the target cancer cells in vivo (Figure 4). In vitro, the internalization was not cell type specific, with all cell types examined indicating high levels of intracellular PI delivery. In vivo, the internalization was dependent on first-pass contact with the RRH prodrug. RRH modification was able to convert PI, a membrane-impermeable intercalator, into a cytotoxic agent by enabling its rapid delivery into cells in vitro under conditions that modeled first-pass therapy (Table 2). The cytotoxicity of the anticancer drug melphalan was also dramatically improved after a similar modification and short-term exposure to cells (Table 2).

The exact nature of the RRH prodrug internalization into the cell is not fully understood at this time. In testing with the stable derivative **IV**, only membrane-associated prodrug was immediately observed after addition to cells (Figure 3F). In cells incubated for 1 hr after delivery of **IV**, punctate staining was observed within the cytoplasm, indicating endocytosis (Figure 3G). Membrane-associated PI was similarly detected immediately after cellular exposure to RRH-PI, by using long camera exposure times. However, in the case of RRH-PI delivery, nuclear PI staining was observed immediately after RRH-PI delivery (within 2 min, Figure 3). Nuclear staining indicates that (a) RRH-PI rapidly inserted into the cell membrane, and that (b) rapid hydrolysis of the hydrophobic modification enabled diffusion of PI to the nucleus. Without the hydrolytic linkage, **IV** remained bound to the cell membranes. In addition, RRH-PI was quickly observed in nuclei in cells kept at 4°C, indicating that the delivery did not require an endocytic step [51] (data not shown). Additional testing

(H) Flow cytometry was conducted on Jurkat cells after treatment with PI (control runs 1–4) and on a suspension of Jurkat cells in ITG, treated with PI (PI runs 1–4) or **II** (II runs 1–4) through the mixing chamber. The results represent a histogram of the relative PI intensity of all single-cell events. (I) Treatment of Hepa 1-6 cells with **II** then Calcein AM to determine live cells (magnification = 200×).

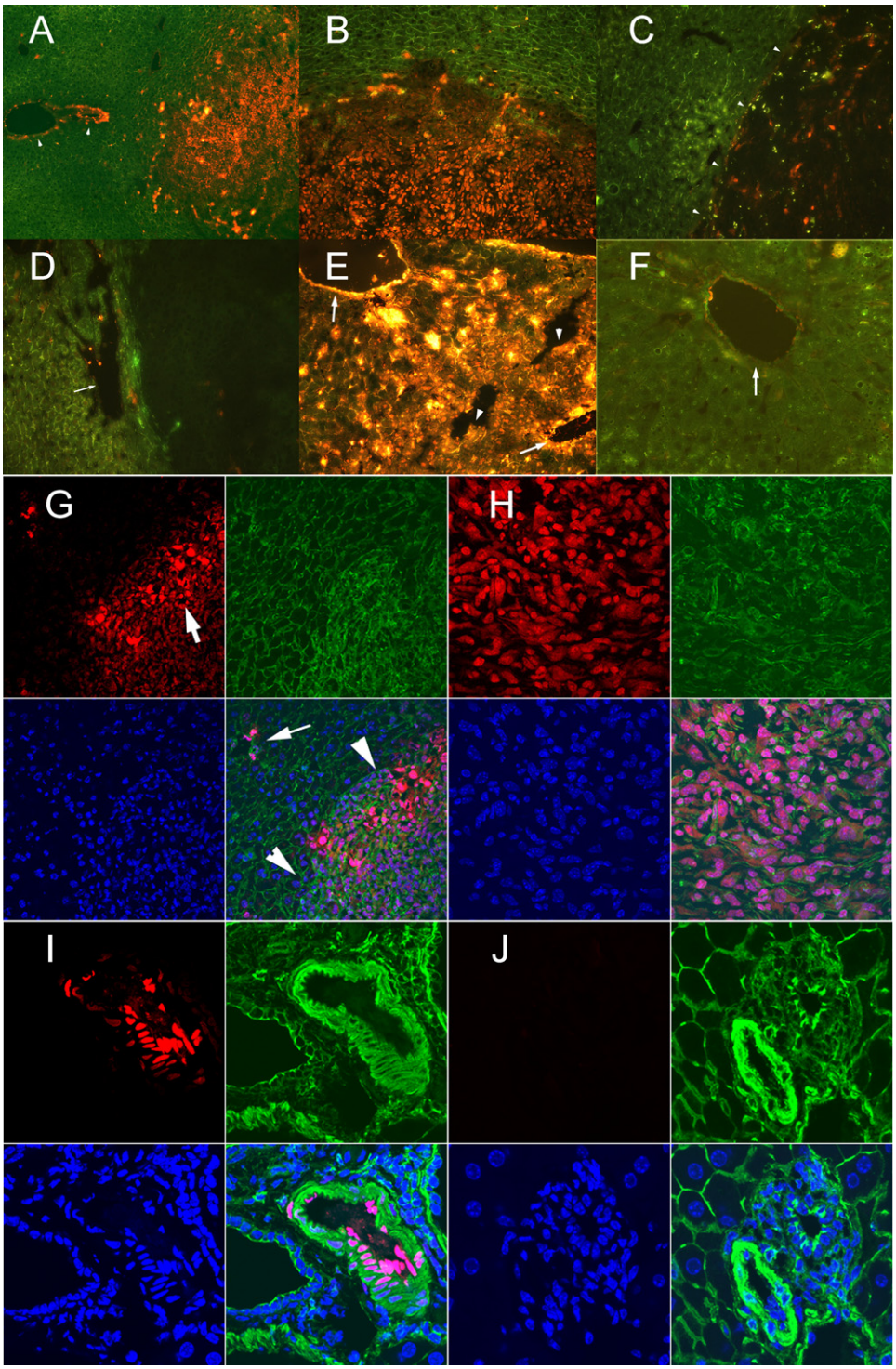

Figure 4. LABI and Portal Vein Delivery of PI and II to C57BL Mice

(A–J) After 3 weeks of MC38 tumor development, PI or **II** (0.150 μmol in 20 μl DMSO, 200 μl ITG) was delivered by LABI or portal vein injections. After 5 min, the livers were harvested, sectioned, and analyzed by fluorescent microscopy (Axioplan-2 fluorescent microscope with FITC emission filter, Zeiss) or stained (green, actin; blue, nuclei) and analyzed by confocal microscopy (Laser LSM 510 confocal microscope, Zeiss). (A) LABI of **II** (magnification = 100×, the arrowhead indicates the hepatic artery and surrounding cells). (B) LABI of **II** (magnification = 200×). (C) LABI of PI (magnification = 200×, the arrowhead indicates the metastases boundary). (D) Portal vein injection with normal blood flow of **II** to a tumor-bearing mouse (magnification = 200×, the arrow indicates the hepatic vein). (E and F) Portal vein injection of (E) **II** to a tumor-bearing mouse or (F) PI to a non-tumor-bearing mouse with the portal vein and celiac artery clamped to occlude blood flow. The blood in the liver was flushed out with 1 ml ITG delivered through the

Table 2. Mean IC_{50} Values for Drug/Prodrug in Various Cell Cultures by Using the WST Assay 24 and 48 hr after Drug Exposure

	Melphalan	V	PI		II		IV	
Cell Type	48 hr	48 hr	24 hr	48 hr	24 hr	48 hr	24 hr	48 hr
Hepa 1-6	>1458[a]	330 (93)	>1,250[b]	>1,700[b]	282 (62)	334 (72)	585 (279)	429 (37)
SKOV-3	>1458[c]	384 (97)	>1,250[b]	>1,700[b]	194 (143)	257 (54)	455 (126)	342 (27)
MC38	1176 (150)	304 (94)						

Cell viability was >90% in cultures exposed to the vehicle alone (DMSO/ITG). IC_{50} values are given as μM, SD.
[a] Cell viability was ~80% of negative control (no treatment) at these maximum concentrations.
[b] Cell viability was >90% of negative control (no treatment) at these maximum concentrations.
[c] Cell viability was ~70% of negative control (no treatment) at these maximum concentrations.

indicated that the internalization was not a result of the DMSO in the procedure [52, 53], nor was it due to generalized membrane damage, and that the cells were viable after treatment.

It is possible that the RRH-PI contacts the cell initially as a micelle, followed by membrane binding similar to detergent insertion into a membrane. The membrane-bound RRH-PI then could enter the cell via a flip mechanism so that PI is internal prior to its hydrolysis [54]. Doxorubicin has been shown to internalize into cells by a flip mechanism with a half-life of minutes [50]. In the case of phospholipids, the rate of flip is generally on the order of hours, although this rate can be more rapid in the presence of polyunsaturated phospholipids and detergents [55]. Therefore, drug internalization due to a flip could be aided by the detergent properties of the prodrug, resulting in a very localized and transient membrane perturbation. For membrane-bound prodrug hydrolyzed prior to internalization, our results suggest that this portion of drug would be lost to the cell given that we were not able to observe a hydrophobic derivative aid in the internalization of another molecule.

A critical test for the RRH prodrug concept involved the ability to demonstrate first-pass delivery to cells in vivo. In a MC38 mouse liver tumor model, LABI with RRH-PI prodrugs resulted in widespread PI staining of the liver tumor cells, while normal liver parenchyma had sparse PI staining (Figure 4). The non-tumor liver cells that were stained were mainly cells of the hepatic artery. Quantitation with confocal microscopy indicated that an average of 94% of the cells in the MC38 metastases were PI positive, while only 2%–3% of the non-tumor cells were PI positive (Figure 4G). No PI-positive cells were observed in other organs, indicating that the RRH-PI had hydrolyzed back to PI prior to contact with other tissues. LABI with PI alone resulted in relatively little PI uptake in tumors and normal liver parenchyma.

Alternatively, when **II** was delivered to the liver via the portal vein with the blood flow temporarily occluded (no clamping on liver outflow), a high percentage of hepatocytes were PI positive (Figure 4E), while the MC38 metastases were relatively PI negative. Intraportal injection of **II** into normal mice resulted in ~70% of the hepatocytes being positive for PI, with ~14% of the administered dose remaining in the liver (compared to 1% of the dose when PI was injected). Although a majority of the PI is still cleared, our results show a dramatic increase in cell uptake.

We therefore tested the efficacy of the RRH-PI prodrug **III** for antitumor response in a mouse MC38 liver metastases model. Survival was significantly ($\rho = 0.02$) prolonged in the **III**-treated group compared to the control group (Figure 5), although it was limited to a few days. Improved survival may be possible by using higher dosing or repeat delivery, as is done with TAC therapy. In the current study, a single injection was employed due to surgical limitations. Although the arterial system was undoubtedly targeted by the RRH prodrug, as evidenced by the fluorescent microscopy studies, no detectable damage was observed; therefore, arterial targeting is unlikely to preclude repeat injections. These results therefore provide proof-of-principle for the use of RRH to enable antitumor effects. Repeat injections, although challenging in a mouse model, would be possible in larger animals, likely leading to ameliorated effects.

SIGNIFICANCE

This report introduces and demonstrates the use of prodrugs with rapidly reversible hydrophobization for improved cellular delivery of the drugs in vitro and in vivo. In this study, designed to serve as a proof-of-concept study, modification of the DNA intercalator PI was conducted. Besides the aforementioned fluorescent properties of PI that were critical to this study, we believed that the electron-withdrawing effect of the phenanthridinium on the exocyclic amines would serve to dramatically destabilize the hydrophobic

portal vein immediately prior to delivery of **II** or PI. Arrows indicate the portal vein; arrowheads indicate the hepatic vein (magnification = 400×). (G) LABI delivery of **II** (magnification = 400×, the arrow indicates a metastatic artery in the rhodamine channel, the arrow indicates the portal tract in the combined view, and the arrowheads indicate the metastasis boundary in the combined view, magnification = 400×). (H) Image from the center of the metastasis from (G) (magnification = 630×). (I) Hepatic artery after LABI delivery of **II** to a non-tumor-bearing mouse (magnification = 630×). (J) Hepatic artery after LABI delivery of PI to a non-tumor-bearing mouse (magnification = 630×).

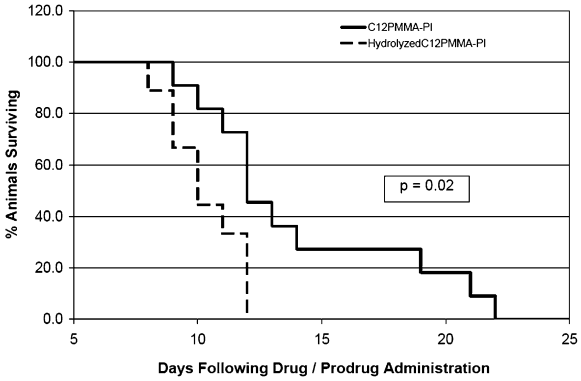

Figure 5. Days of Survival after LABI Delivery of C12PMMA-PI or Hydrolyzed C12PMMA-PI to C57BL Mice

After 3 weeks of MC38 tumor development, C12PMMA-PI or hydrolyzed C12PMMA-PI (0.150 μmol in 20 μl DMSO, 200 μl ITG) was delivered by LABI. The mouse abdomen was closed 4 min after drug treatment, and the animals were monitored for survival time.

derivatives toward hydrolysis. This was realized, as RRH-PI prodrugs possess half-lives on the order of 10–20 s. Labile hydrophobization induced cellular internalization of PI by a rapid, non-endocytosis-driven mechanism. Remote tissues were protected from the highly active prodrugs due to the rapid lability of the hydrophobic moiety.

In general terms, depending on the functional group modified, and the type of attachment linkage used, it should be possible to regulate the hydrolysis rate of the prodrug, and therefore the active lifetime of the prodrug for a desired treatment application. Although this idea poses a very significant synthetic challenge, our results with the delivery of PI have demonstrated that this methodology allows for the development of active therapeutics from cell-impermeable compounds, potentially leading to therapeutics possessing low systemic toxicity. Although the hydrolytic instability of the RRH-PI prodrugs necessitated the use of DMSO in the injection solution, alternative mechanisms for lability could potentially be developed, such as rapid change in pH, thereby avoiding the use of DMSO. Overall, this approach is particularly applicable to first-pass treatment strategies, most notably those involving liver tumors or ovarian cancer. However, any tumor or organ that has an identifiable vascular source could potentially be targeted, and it therefore provides an exciting avenue to improve chemotherapeutics for a variety of cancers and other disorders.

EXPERIMENTAL PROCEDURES

All chemical reactions were carried out in a nitrogen or argon atmosphere by using flame-dried glassware. Anhydrous N,N-dimethylformamide (DMF, Aldrich) and anhydrous dimethyl sulfoxide (DMSO, Aldrich) were used without further purification. Potassium carbonate (Aldrich) and molecular sieves (3 Å, Aldrich) were flame dried under vacuum prior to use. Propidium iodide (PI, 95%, Aldrich) was used without further purification. ^{1}H-NMR spectroscopy was performed on a Bruker AC+ 250, a Bruker AC+ 300, or a Varian Unity INOVA 400 spectrometer. Mass analysis was conducted on a PE Sciex API 150EX mass spectrometer. Cells were purchased from ATCC (Manassas, VA), unless otherwise noted, and cultured according to the distributor's instructions. Complete details on prodrug hydrolysis and particle sizing can be found in the Supplemental Data available with this article online.

Compound Preparation and Lability

N-Dodecyl-3-(4-methyl-2,5-dioxo-2,5-dihydro-furan-3-yl)-propionamide, C12PMMA

To a solution of 3-(4-methyl-2,5-dioxo-2,5-dihydro-furan-3-yl)-propionic acid [41] (800 mg, 4.34 mmol) in dichloromethane (22 ml) was added oxalyl chloride (0.41 ml, 4.56 mmol, Aldrich) dropwise under nitrogen. The resulting solution was stirred at ambient temperature for 6 hr and concentrated under reduced pressure. The resulting oil was suspended in dichloromethane (22 ml), and dodecyl amine (1.10 ml, 4.78 mmol, Aldrich), followed by diisopropylethylamine (0.83 ml, 4.78 mmol, Aldrich), was added. After 4 hr, the solution was concentrated under reduced pressure. The resulting reside was taken up in EtOAc (150 ml), washed twice with HCl (20 ml, 1 N), washed once with H_20, dried (Na_2SO_4), filtered, and concentrated to afford a white solid. The solid was purified by flash chromatography on silica gel (40 × 160 mm, EtOAc/Hexanes 1:1 eluent) to afford 1.04 g C12PMMA (68%) as a white solid. 400 MHz ^{1}H-NMR ($CDCl_3$, 99.8%, ppm) δ 5.720 (1H, s) 3.20 (2H, dt, J = 6.4, 7.0) 2.79 (2H, t, J = 7.0) 2.530 (2H, t, J = 7.0) 2.13 (3H, s) 1.55–1.42 (2H, m) 1.34–1.24 (18H, m) 0.88 (3H, t, J = 7.0). ^{13}C-NMR ($CDCl_3$, 99.8%, ppm) δ170.509, 166.194, 166.156, 143.007, 142.465, 39.974, 33.093, 32.116, 29.832, 29.786, 29.756, 29.733, 29.549, 29.481, 27.106, 22.890, 20.645, 14.321, 9.876. Molecular ion + 1 calculated for $C_{20}H_{33}NO_4$ = 352.2, found m/e = 352.2.

Synthesis of 3,8-Bis([(dimethyl)octadecylsilazyl] Amine) 5-(3,3-Diethyl-3-methylammonium Propyl) 6-Phenyl Phenanthridinium Diiodide, II

To PI, chloro(dimethyl)octadecylsilane (6 eq., 95%, Aldrich), K_2CO_3 (10 eq.), and molecular sieves (3 Å, 10 wt eq.) was added anhydrous DMF or DMSO (7.5–15 μmol/ml final concentration). The resulting suspension was heated at 60°C for 12 hr, cooled to ambient temperature, centrifuged, filtered (0.2 μm Nylon membrane) under inert atmosphere, and precipitated in diethyl ether to afford **II** as a purple solid. 300 MHz NMR (N,N-dimethylformamide-d7, 99.5%, ppm) δ 8.72 (2H, dd, J = 9.2, 6.6) 8.38 (1H, d, J = 1.7) 7.93–7.80 (5H, m) 7.74 (1H, dd, J = 9.1, 2.3) 7.48 (1H, dd, J = 9.1, 1.7) 6.66 (1H, s) 6.46 (1H, d, J = 2.3) 6.13 (1H, s) 4.59 (2H, m) 4.66–4.55 (2H, m) 3.88–3.75 (2H, m) 3.58–3.40 (2H, q, J = 7.2) 3.21 (3H, s) 2.62–2.45 (2H, m) 1.40–1.18 (70H, m) 0.90–0.84 (6H, m) 0.55–0.49 (4H, m) 0.3 (12H, s). In DMSO, λ_{ex} max = 460 nm, λ_{em} max = 638 nm.

In some preparations, ^{1}H-NMR analysis indicated the formation two additional compounds as minor components in the reaction mixture (<10%). A trisilylated PI was observed (based on integration), arising from two silylation reactions taking place on one of the PI amino groups. The second minor component was identified as the phenanthridinium salt of **II** (verified by independent synthesis, from the reaction of PI and chloro(dimethyl)octadecylsilane in dichloromethane in the absence of a base).

Synthesis of 3,8-Bis-(2-[2 Carboxyethylidene]-4-[dodecarbamoyl]-1-oxo-butylamine) 5-(3,3-Diethyl-3-methylammonium Propyl) 6-Phenyl Phenanthridinium Diiodide, III

To PI, C12PMMA (3 eq.), K_2CO_3 (10 eq.), and molecular sieves (3 Å, 10 wt eq.) was added anhydrous DMF or DMSO (7.5–15 μmol/ml final concentration). The resulting suspension was heated at 60°C for 12 hr, cooled to ambient temperature, centrifuged, filtered (0.2 μm Nylon membrane) under inert atmosphere, and precipitated in diethyl ether to afford **III** as a mixture of isomers. Further attempts to purify **III**

lead to a rapid hydrolysis of the maleamic acid and regeneration of PI. 300 MHz NMR (Dimethyl sulfoxide-d6, 99.5%, ppm) δ 8.64 (2H, dd, *J* = 9.2, 8.2) 7.79–7.74 (5H, m) 7.56 (1H, dd, *J* = 9.2, 2.3) 7.41–7.29 (2H, m) 7.24–7.14 (1H, m) 6.67–6.62 (1 H, br m) 6.24 (1H, d, *J* = 2.3) 6.02–5.96 (2H, br) 4.43–4.33 (2H, br m) 3.45–2.70 (21H, m) 2.40–1.85 (8H, m) 1.52–0.98 (46H, m) 0.87–0.80 (6H, m). In DMSO, λ_{ex} max = 460 nm, λ_{em} max = 635 nm.

Synthesis of 3,8-Bis-undecylcarbanylamino 5-(3,3-Diethyl-3-methylammonium Propyl) 6-Phenyl Phenanthridinium Diiodide, IV

To PI (36.1 mg, 0.0540 mmol, Aldrich) in dichloromethane (10 ml) was added lauroyl chloride (26.9 μl, 0.113 mmol, 2.1 eq., Aldrich), followed by diisopropylethylamine (20.7 μl, 0.119 mmol, 2.2 eq., Aldrich). The resulting solution was stirred at ambient temperature for 16 hr and then partitioned in EtOAc/H_20, washed twice with H_20, washed once with brine, dried (Na_2SO_4), filtered, and concentrated. The resulting yellow solid was crystallized twice from acetonitrile to afford 53.7 mg (96%) **IV**. Molecular ion calculated for $C_{51}H_{78}N_4O_2I$ = 905.5, found m/e = 905.7, molecular ion/2 calculated for $C_{51}H_{78}N_4O_2$ = 389.6, found m/e = 389.9. 400 MHz ^{1}H-NMR (Dimethyl sulfoxide-d6, 99.5%, ppm) δ 11.80 (1H, s) 10.74 (1H, s) 9.16 (1H, s) 9.11 (1H, d, *J* = 9.6) 9.06 (1H, d, *J* = 9.2) 8.62 (1H, d, *J* = 8.8) 8.48 (1H, dd, *J* = 9.2, 2.0) 8.02 (1H, d, *J* = 2.0) 7.85–7.74 (5H, m) 4.63–4.52 (2H, m) 3.33–3.25 (6H, m) 2.94 (3H, s) 2.42–2.28 (4H, m) 2.19–2.16 (2H, m) 1.68–1.45 (4H, m) 1.40–1.15 (38H, m) 0.85 (6H, t *J* = 5.8). In H_2O, λ_{ex} max = 443 nm, λ_{em} max = 546 nm.

Synthesis of 3,9-Diaza, 2-(4-[bis(2-chloroethyl)amino] Phenyl Methyl), 5-(2-Carboxyl Ethylidine), 4,8-Dioxo Uncosanoic Acid, V

To melphalan (18.2 mg, 0.0596 mmol, Sigma), C12PMMA (41.9 mg, 0.119 mmol), K_2CO_3 (8.3 mg, 0.060 mmol), and molecular sieves (3 Å, 182 mg) was added anhydrous DMSO (1.82 ml). The resulting suspension was heated at 60°C for 12 hr, cooled to ambient temperature, centrifuged, and filtered (0.2 μm membrane) under inert atmosphere, to afford **V** as a mixture of isomers. Molecular ion + 1 calculated for $C_{33}H_{51}N_3O_6Cl_2$ = 656.3, found m/e = 655.5. Molecular ion − 1 calculated for $C_{33}H_{51}N_3O_6Cl_2$ = 654.3, found m/e = 636.3 (M-1-18). 400 MHz NMR (Dimethyl sulfoxide-d6, 99.5%, ppm) δ 7.94–7.72 (2H, m) 6.90 (2H, d, J_{AB} = 8.6) 6.57 (2H, d, J_{AB} = 8.6) 4.16 (1H, m) 3.72–3.50 (8H, m) 3.323–3.181 (2H, m) 2.99–2.96 (2H, m) 2.48–2.44 (0.8H, m) 2.21 (1.2H, t, *J* = 7.4) 1.92 (1H, s) 1.81 (2H, s) 1.38–1.23 (20H, m) 0.85 (3H, t, *J* = 6.8).

In Vitro Cellular Uptake

Fluorescent microscopy studies were conducted with a three-laser LSM 510 confocal microscope, an Axiovert S100 fluorescent microscope, or an Axioplan-2 fluorescent microscope (all Zeiss) equipped with filter sets for the rhodamine fluorescence channel (λex = BP 450/12, λem = LP 590 nm filter set) and the fluorescein fluorescent channel (λex = BP 546/90, λem = LP 515 nm filter set). Imaging was performed with an AxioCam digital camera (Zeiss), with AxioVision imaging software (V 4.5, Zeiss). For all images, identical camera settings and exposure times were used on comparative sample and control images. Images were processed with Photoshop (Adobe) for level and brightness by using identical settings between sample and control images.

Adherent cells were plated at 2.5 × 10^5 cells/well on 6-well plates 24 hr prior to testing. Details for the treatment of suspension cells, including flow cytometry, can be found in the Supplemental Data. The growth media were removed from individual wells, and the drug/prodrug was immediately added to the well with the mixing chamber. Detailed information for the construction and use of the mixing chamber can be found in the Supplemental Data. Final drug/prodrug concentrations were 0.150 μmol in 220 μl total volume (20 μl OS, 200 μl ITG). After 30 s, the drug solution was removed (aspirated), and 2 ml complete media was added to the cells. Each condition was repeated in two or three wells, and the cells were immediately examined by fluorescent microscopy. Experiments conducted with prodrug that was hydrolyzed prior to application to the cells followed a similar protocol; however, the mixed solution was aged for 5 min prior to testing. Cell viability experiments followed a similar protocol for drug treatment (4 min). Calcein AM and SYTOX Green (both Invitrogen) were used according to the manufacturer's instructions.

For experiments conducted with **IV**, the cells were plated on 6-well plates with coverslips. After treatment as described above, the coverslip was removed and inverted over one drop of media on a glass slide for imaging. PI was also mixed with **IV** or **V** and then delivered to Hepa 1-6 and SKOV-3 cells. Mixing procedures can be found in the Supplemental Data.

Antiproliferative/Cytotoxic In Vitro Studies

In vitro cytotoxicity testing was conducted on Hepa 1-6 (mouse hepatoma), SKOV-3 (human ovarian carcinoma), and MC38 (mouse colon carcinoma) cells by using a tetrazolium-based assay (WST-1, Dojindo Molecular Technologies) [56]. For the WST assay, Hepa 1-6 (2.0 × 10^5 cells well), SKOV-3 (7.5 × 10^5 cells well), and MC38 (8.5 × 10^5 cells well) cells were seeded in 1 ml media into 12-well plates 24 hr prior to testing (starting confluency of 50%). After removal of media, a drug/prodrug solution was added dropwise to quadruplicate wells, by using the mixing chamber. Effective drug concentrations were calculated from the amount of drug added in the total volume of OS and aqueous solution. After 4 min of exposure, the drug solution was removed, and 1 ml media was added to each well. After a 24–48 hr incubation, WST-1 (20 μl 5 mM solution in PBS) and N-methylphenazonium methyl sulfate (PMS, 20 μl 0.2 mM solution in PBS) were added, and the cells were incubated for 1–4 hr. For MC38 cells, the amounts of WST-1 and PMS were doubled. After incubation, 100 μl sample was transferred to quadruplicate wells on a 96-well plate, and the absorbance (438 nm) values were measured on a SPECTRAmax Plus^{384} microplate spectrophotometer (Molecular Devices Corporation). Data represent the mean A438 values of 16 wells, corrected for media contribution and normalized against cells in media with no drug/prodrug treatment (reported as percent cell viability ±SD). The concentration of drug (μM) that is required for 50% inhibition in vitro is reported as the IC_{50} (±SD) and was calculated from the best-fit line (Excel) for a plot of effective drug concentration against percent cell viability.

In Vivo Studies

All animal experiments were performed in accordance with Institutional Animal Care and Use Committee protocols. All surgical procedures were performed under Isoflurane anesthesia and with a dissection microscope (MZ-6, Leica, Germany). A complete list of tumor models and methods can be found in the Supplemental Data.

Drug/prodrug solutions (as described above) were delivered with the mixing chamber via a liver arterial bolus injection (LABI) to the right gastroduodenal artery (35 gauge needle) for retrograde delivery to the hepatic artery, similar to procedures used clinically [57]. A complete description of the experimental procedure can be found in Supplemental Data. For confocal microscopy, the livers were harvested 5 min after LABI, snap frozen in O.C.T. compound, cryosectioned, and stained (for confocal, green, actin [Alexa 488]; blue, nuclei [ToPro-3]). Unstained sections of the same liver were examined by fluorescent microscopy with both rhodamine and long-pass FITC emission filters (505 plus) in order to observe the low-magnification signaling pattern (green signal is autofluorescence). For experiments designed to determine the number of PI-positive cells, five random fields of liver tumors and five fields containing portal triad's free of tumor were imaged. The total number of cells and positive cells were counted to determine the percentage of positive cells in the corresponding regions. For experiments designed to monitor the antitumor effects of the prodrugs, **III** (n = 11) or hydrolyzed **III** (n = 9) was injected as previously described, the mouse abdomen was closed after drug treatment, and the animals were monitored for survival time. Statistical analysis was conducted by using a t test (two-tailed distribution and two sample, unequal variance, Excel).

For intraportal injections, both the portal vein and the celiac artery were clamped to occlude blood flow into the liver. In other experiments, the portal vein and the celiac artery were not clamped, preserving full portal blood flow during the experiment. In all cases, the vena cava was not clamped in order to avoid increased pressure within the liver. For experiments with occluded blood flow, the blood in the liver was flushed out with 1 ml ITG delivered through the portal vein (1 min). Then, 0.300 μmol PI or **II** in 40 μl DMF was delivered together with 400 μl ITG via the mixing chamber. Five minutes after injection, the livers were perfused with 3 ml ITG to flush any drug remaining in the vasculature, and livers were cryosectioned as described above, or the hepatocytes were isolated [58]. Experimental details for nucleic acid isolation and analysis from hepatocytes can be found in the Supplemental Data.

The effect of drug/prodrug treatment was also evaluated on proliferating hepatocytes after a 70% partial hepatectomy on normal ICR mice [59]. After the hepatectomy, drug/prodrug (0.150 μmol, 220 μl total injection volume) was delivered to the liver via the portal vein by using the mixing chamber. After 48 hr, the animals were sacrificed, and the livers were harvested, formalin fixed, paraffin embedded, sectioned, and H&E stained. A total of 50 random parenchymal fields per animal were examined, and the number of hepatocyte mitotic figures (metaphase) was determined together with the total number of hepatocytes (~2000 per animal). Results are reported as the percentage of cells in metaphase (±SD).

Supplemental Data

Supplemental Data include Supplemental Experimental Procedures used in this work and are available at http://www.chembiol.com/cgi/content/full/14/9/1065/DC1/.

ACKNOWLEDGMENTS

During the preparation of this manuscript, we lost our dear friend and colleague, Vladimir Budker. Vladimir was an outstanding person and scholar, and he will be deeply missed. We dedicate this report to his memory. The authors would like to thank Stephanie Bertin for tissue culture work, Brian Hughes for flow cytometry experiments, David Rozema and Darren Wakefield for helpful discussions on prodrug lability, Lisa Nader and Brian Pujanauski for a preparation of C12PMMA, and Andrei Blokhin and Kirk Ekena for helpful suggestions regarding the preparation of this manuscript. The authors also wish to acknowledge Dr. Thomas C. Stringfellow, and the Analytical Instrumentation Center of the School of Pharmacy, UW-Madison, for access and support in obtaining NMR data. S.D.M., V.M.S., P.M.S., Z.C.N., and H.H. are or were employees of Mirus Bio Corporation. V.G.B. and J.A.W. are founders of Mirus Bio Corporation.

Received: February 5, 2007
Revised: August 6, 2007
Accepted: August 10, 2007
Published: September 21, 2007

REFERENCES

1. Reddy, L.H. (2005). Drug delivery to tumours: recent strategies. J. Pharm. Pharmacol. *57*, 1231–1242.
2. Jaracz, S., Chen, J., Kuznetsova, L.V., and Ojima, L. (2005). Recent advances in tumor-targeting anticancer drug conjugates. Bioorg. Med. Chem. *13*, 5043–5054.
3. Kidane, A., and Bhatt, P.P. (2005). Recent advances in small molecule drug delivery. Curr. Opin. Chem. Biol. *9*, 347–351.
4. Andresen, T.L., Jensen, S.S., and Jorgensen, K. (2005). Advanced strategies in liposomal cancer therapy: problems and prospects of active and tumor specific drug release. Prog. Lipid Res. *44*, 68–97.
5. Torchilin, V.P. (2005). Recent advances with liposomes as pharmaceutical carriers. Nat. Rev. Drug Discov. *4*, 145–160.
6. Nori, A., and Kopecek, J. (2005). Intracellular targeting of polymer-bound drugs for cancer chemotherapy. Adv. Drug Deliv. Rev. *57*, 609–636.
7. Qiu, L.Y., and Bae, Y.H. (2006). Polymer architecture and drug delivery. Pharm. Res. *23*, 1–30.
8. Soyez, H., Schacht, E., and Vanderkerken, S. (1996). The crucial role of spacer groups in macromolecular prodrug design. Adv. Drug Deliv. Rev. *21*, 81–106.
9. Le Garrec, D., Ranger, M., and Leroux, J.C. (2004). Micelles in anticancer drug delivery. Am. J. Drug Deliv. *2*, 15–42.
10. Gaucher, G., Dufresne, M.H., Sant, V.P., Kang, N., Maysinger, D., and Leroux, J.C. (2005). Block copolymer micelles: preparation, characterization and application in drug delivery. J. Control. Release *109*, 169–188.
11. Dufresne, M.H., Garrec, D.L., Sant, V., Leroux, J.C., and Ranger, M. (2004). Preparation and characterization of water-soluble pH-sensitive nanocarriers for drug delivery. Int. J. Pharm. *277*, 81–90.
12. Zhi, P.X., Qing, H.Z., Gao, Q.L., and Ai, B.Y. (2006). Inorganic nanoparticles as carriers for efficient cellular delivery. Chem. Eng. Sci. *61*, 1027–1040.
13. Dreher, M.R., Liu, W., Michelich, C.R., Dewhirst, M.W., Yuan, F., and Chilkoti, A. (2006). Tumor vascular permeability, accumulation, and penetration of macromolecular drug carriers. J. Natl. Cancer Inst. *98*, 335–344.
14. Shen, W.C., and Ryser, H.J. (1981). cis-Aconityl spacer between daunomycin and macromolecular carriers: a model of pH-sensitive linkage releasing drug from a lysosomotropic conjugate. Biochem. Biophys. Res. Commun. *102*, 1048–1054.
15. Ulbrich, K., and Subr, V. (2004). Polymeric anticancer drugs with pH-controlled activation. Adv. Drug Deliv. Rev. *56*, 1023–1050.
16. El-Serag, H.B., and Mason, A.C. (1999). Rising incidence of hepatocellular carcinoma in the United States. N. Engl. J. Med. *340*, 745–750.
17. Holen, K.D., and Saltz, L.B. (2001). New therapies, new directions: advances in the systemic treatment of metastatic colorectal cancer. Lancet Oncol. *2*, 290–297.
18. Iwatsuki, S., Dvorchik, I., Madariaga, J.R., Marsh, J.W., Dodson, F., Bonham, A.C., Geller, D.A., Gayowski, T.J., Fung, J.J., and Starzl, T.E. (1999). Hepatic resection for metastatic colorectal adenocarcinoma: a proposal of a prognostic scoring system. J. Am. Coll. Surg. *189*, 291–299.
19. Pinson, C.W., Wright, J.K., Chapman, W.C., Garrard, C.L., Blair, T.K., and Sawyers, J.L. (1996). Repeat hepatic surgery for colorectal cancer metastasis to the liver. Ann. Surg. *223*, 765–773.
20. Dmitrewski, J., El-Gazzaz, G., and McMaster, P. (1998). Hepatocellular cancer: resection or transplantation. J. Hepatobiliary Pancreat. Surg. *5*, 18–23.
21. Kemeny, N., Huang, Y., Cohen, A.M., Shi, W., Conti, J.A., Brennan, M.F., Bertino, J.R., Turnbull, A.D., Sullivan, D., Stockman, J., et al. (1999). Hepatic arterial infusion of chemotherapy after resection of hepatic metastases from colorectal cancer. N. Engl. J. Med. *341*, 2039–2048.
22. Ikeda, M., Maeda, S., Shibata, J., Muta, R., Ashihara, H., Tanaka, M., Fujiyama, S., and Tomita, K. (2004). Transcatheter arterial chemotherapy with and without embolization in patients with hepatocellular carcinoma. Oncology *66*, 24–31.
23. Trevisani, F., De Notariis, S., Rossi, C., and Bernardi, M. (2001). Randomized control trials on chemoembolization for hepatocellular carcinoma: is there room for new studies? J. Clin. Gastroenterol. *32*, 383–389.
24. Ramsey, D.E., Kernagis, L.Y., Soulen, M.C., and Geschwind, J.F. (2002). Chemoembolization of hepatocellular carcinoma. J. Vasc. Interv. Radiol. *13*, S211–S221.

25. Venook, A.P., and Warren, R.S. (2001). Therapeutic approaches to metastasis confined to the liver. Curr. Oncol. Rep. *3*, 109–115.
26. Pentecost, M.J. (1993). Transcatheter treatment of hepatic metastases. AJR Am. J. Roentgenol. *160*, 1171–1175.
27. Archer, S.G., and Gray, B.N. (1989). Vascularization of small liver metastases. Br. J. Surg. *76*, 545–548.
28. Laffer, U.T., and Metzger, U. (1995). Intraportal chemotherapy for colorectal hepatic metastases. World J. Surg. *19*, 246–251.
29. Young, A.M., Daryanani, S., and Kerr, D.J. (1999). Can pharmacokinetic monitoring improve clinical use of fluorouracil? Clin. Pharmacokinet. *36*, 391–398.
30. Ensminger, W.D., Rosowsky, A., Raso, V., Levin, D.C., Glode, M., Come, S., Steele, G., and Frei, E., 3rd. (1978). A clinical-pharmacological evaluation of hepatic arterial infusions of 5-fluoro-2′-deoxyuridine and 5-fluorouracil. Cancer Res. *38*, 3784–3792.
31. Kerr, D.J., McArdle, C.S., Ledermann, J., Taylor, I., Sherlock, D.J., Schlag, P.M., Buckels, J., Mayer, D., Cain, D., and Stephens, R.J. (2003). Intrahepatic arterial versus intravenous fluorouracil and folinic acid for colorectal cancer liver metastases: a multicentre randomised trial. Lancet *361*, 368–373.
32. Garnier-Suillerot, A., Marbeuf-Gueye, C., Salerno, M., Loetchutinat, C., Fokt, I., Krawczyk, M., Kowalczyk, T., and Priebe, W. (2001). Analysis of drug transport kinetics in multidrug-resistant cells: implications for drug action. Curr. Med. Chem. *8*, 51–64.
33. Wender, P.A., Mitchell, D.J., Pattabiraman, K., Pelkey, E.T., Steinman, L., and Rothbard, J.B. (2000). The design, synthesis, and evaluation of molecules that enable or enhance cellular uptake: peptoid molecular transporters. Proc. Natl. Acad. Sci. USA *97*, 13003–13008.
34. McKeage, M.J., Berners-Price, S.J., Galettis, P., Bowen, R.J., Brouwer, W., Ding, L., Zhuang, L., and Baguley, B.C. (2000). Role of lipophilicity in determining cellular uptake and antitumour activity of gold phosphine complexes. Cancer Chemother. Pharmacol. *46*, 343–350.
35. Zidek, Z., Kmonickova, E., and Holy, A. (2005). Cytotoxicity of pivoxil esters of antiviral acyclic nucleoside phosphonates: adefovir dipivoxil versus adefovir. Biomed. Pap. Med. Fac. Univ. Palacky Olomouc Czech Repub. *149*, 315–319.
36. Holford, N.H.G. (2007). Pharmacokinetics & Pharmacodynamics: Rational Dosing & the Time Course of Drug Action. In Basic & Clinical Pharmacology, B.G. Katzung, ed. (New York: The McGraw-Hill Companies), pp. 34–49.
37. Brana, M.F., Cacho, M., Gradillas, A., de Pascual-Teresa, B., and Ramos, A. (2001). Intercalators as anticancer drugs. Curr. Pharm. Des. *7*, 1745–1780.
38. Martinez, R., and Chacon-Garcia, L. (2005). The search of DNA-interealators as antitumoral drugs: what it worked and what did not work. Curr. Med. Chem. *12*, 127–151.
39. Luedtke, N.W. (2003). RNA affinity and specificity of modified aminoglycosides, metal complexes, and intercalating agents that target the HIV-1 Rev response element. PhD thesis, University of California, San Diego, California.
40. Prout, T.R., Thompson, M.L., Haltiwanger, R.C., Schaeffer, R., and Norman, A.D. (1994). New skeletally stabilized silazanes and siloxazanes. Inorg. Chem. *33*, 1778–1782.
41. Rozema, D.B., Ekena, K., Lewis, D.L., Loomis, A.G., and Wolff, J.A. (2003). Endosomolysis by masking of a membrane-active agent (EMMA) for cytoplasmic release of macromolecules. Bioconjug. Chem. *14*, 51–57.
42. Shen, W.C., and Heiati, H. (2003). Reversible aqueous pH sensitive lipidizing reagents, compositions and methods of use. July 2003. U.S. patent 6,590,071.
43. Wang, J., Hogenkamp, D.J., Tran, M., Li, W.Y., Yoshimura, R.F., Johnstone, T.B., Shen, W.C., and Gee, K.W. (2006). Reversible lipidization for the oral delivery of leu-enkephalin. J. Drug Target. *14*, 127–136.
44. Fasman, G.D. (1975). Handbook of Biochemistry and Molecular biology, Third Edition (Cleveland: CRC Press).
45. Hessel, V., Lowe, H., and Schonfeld, F. (2005). Micromixers—a review on passive and active mixing principles. Chem. Eng. Sci. *60*, 2479–2501.
46. Pabit, S.A., and Hagen, S.J. (2002). Laminar-flow fluid mixer for fast fluorescence kinetics studies. Biophys. J. *83*, 2872–2878.
47. Rodriguez-Vicente, J., Vicente-Ortega, V., and Canteras-Jordana, M. (1998). The effects of different antineoplastic agents and of pretreatment by modulators on three melanoma lines. Cancer *82*, 495–502.
48. Alpini, G., Phillips, J.O., and Larusso, N.F. (1994). The biology of biliary epithelia. In The Liver: Biology and Pathobiology, Third Edition, I.M. Arias, ed. (New York: Raven Press), pp. 623–664.
49. Sebestyen, M.G., Budker, V.G., Budker, T., Subbotin, V.M., Zhang, G., Monahan, S.D., Lewis, D.L., Wong, S.C., Hagstrom, J.E., and Wolff, J.A. (2006). Mechanism of plasmid delivery by hydrodynamic tail vein injection. I. Hepatocyte uptake of various molecules. J. Gene Med. *8*, 852–873.
50. Regev, R., and Eytan, G.D. (1997). Flip-flop of doxorubicin across erythrocyte and lipid membranes. Biochem. Pharmacol. *54*, 1151–1158.
51. Mukherjee, S., Ghosh, R.N., and Maxfield, F.R. (1997). Endocytosis. Physiol. Rev. *77*, 759–803.
52. Swanson, B.N. (1985). Medical use of dimethyl sulfoxide (DMSO). Rev. Clin. Basic Pharm. *5*, 1–33.
53. Montaguti, P., Melloni, E., and Cavalletti, E. (1994). Acute intravenous toxicity of dimethyl sulfoxide, polyethylene glycol 400, dimethylformamide, absolute ethanol, and benzyl alcohol in inbred mouse strains. Arzneimittelforschung *44*, 566–570.
54. Armstrong, V.T., Brzustowicz, M.R., Wassall, S.R., Jenski, L.J., and Stillwell, W. (2003). Rapid flip-flop in polyunsaturated (docosahexaenoate) phospholipid membranes. Arch. Biochem. Biophys. *414*, 74–82.
55. Pantaler, E., Kamp, D., and Haest, C.W. (2000). Acceleration of phospholipid flip-flop in the erythrocyte membrane by detergents differing in polar head group and alkyl chain length. Biochim. Biophys. Acta *1509*, 397–408.
56. Ishiyama, M., Tominaga, H., Shiga, M., Sasamoto, K., Ohkura, Y., and Ueno, K. (1996). A combined assay of cell viability and in vitro cytotoxicity with a highly water-soluble tetrazolium salt, neutral red and crystal violet. Biol. Pharm. Bull. *19*, 1518–1520.
57. Kemeny, M.M. (2001). The surgical aspects of the totally implantable hepatic artery infusion pump. Arch. Surg. *136*, 348–352.
58. Klaunig, J.E., Goldblatt, P.J., Hinton, D.E., Lipsky, M.M., Chacko, J., and Trump, B.F. (1981). Mouse liver cell culture. I. Hepatocyte isolation. In Vitro *17*, 913–925.
59. Braun, K.M., and Sandgren, E.P. (2000). Cellular origin of regenerating parenchyma in a mouse model of severe hepatic injury. Am. J. Pathol. *157*, 561–569.